Macromolecules

pubs.acs.org/Macromolecules Article

Unifying Step-Growth Polymerization and On-Demand Cascade Ring-Closure Depolymerization via Polymer Skeletal Editing

Fabiana Siragusa, Jeremy Demarteau, Thomas Habets, Ion Olazabal, Koen Robeyns, Gwilherm Evano, Raphael Mereau, Thierry Tassaing, Bruno Grignard,* Haritz Sardon, and Christophe Detrembleur*

Cite This: *Macromolecules* 2022, 55, 4637−4646 Read Online

ACCESS | Metrics & More | Article Recommendations | Supporting Information

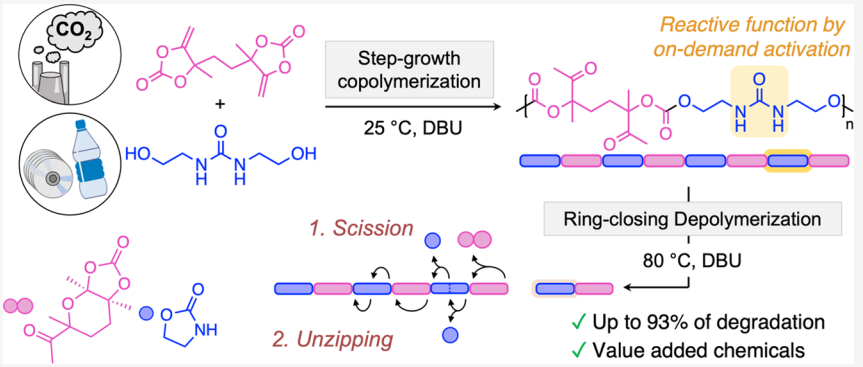

ABSTRACT: The inherent skeletal and thermal features to forge polymers by step-growth polymerization are conflicting with any depolymerization strategies via cascade back-biting reactions that necessitate adequate ceiling temperature, spacers, and functionalities to create cyclic compounds. Here, we report the edition of step-growth poly(carbonate-urea)s and poly(carbonate-amide)s that are depolymerized on demand into their native precursor or added-value offspring oxazolidinones, together with a hemiacetal cyclic carbonate. The unprotected in-chain secondary amide or urea functionalities of the polymers trigger their degradation via cascade ring-closing events upon a thermal switch (from 25 to 80 °C) in the presence of an organic base as a catalyst. Although most studies are realized in solution for understanding the deconstruction process, the polymers are also fully degraded in 2 h in neat conditions without any catalyst at 150 °C. At 80 °C, the organic base is required to accelerate the process. On the road to sustainability and circularity, we validate the concept by exploiting monomers designed from waste CO_2 and upcycled commodity plastics. Ultimately, these polymers are selectively depolymerized from plastic mixtures composed of commodity poly(ethylene terephthalate) and polycaprolactone, offering new options for recycling plastic waste mixtures while delivering high-value-added chemicals.

INTRODUCTION

Over the last century, commodities of engineered plastics have totally reshaped our modern life. Their ever-growing utilization coupled with the lack of viable end-of-life scenarios, finite fossil origin, and long-term persistence in marine ecosystems and nature are now causing a major environmental crisis.[1,2] This has pushed scientists to fundamentally reinvent the way to fabricate, use, and recycle, ideally on-demand, these materials in a circular, sustainable, and economic manner.[3−22] Circular economy of plastics is better achieved through chemical recycling, where the polymer chain is depolymerized into the pristine monomer or new value-added chemicals. In this context, heteroatom-linked step-growth polymers such as polyesters, polyurethanes, and polycarbonates can play a pivotal role in tackling the plastic pollution problem. The presence of in-chain C−O or C−N labile bonds offers various chemical depolymerization opportunities via solvolysis, producing either the initial monomers that are re-employed in a closed-loop system or, new added-value chemicals via an open-loop upcycling approach.[8,10] Developing creative and energy-efficient deconstruction strategies, beyond solvolysis, to enlarge and diversify the scope of accessible chemicals from step-growth polymers represents an exciting but rather unexplored research area.

Ring-closing depolymerization is a powerful method to transform polymer backbones into cyclic products, yet is made virtually applicable to all polyesters and polycarbonates

Received: April 5, 2022
Revised: May 6, 2022
Published: June 1, 2022

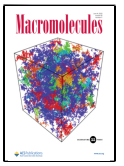

https://doi.org/10.1021/acs.macromol.2c00696
Macromolecules 2022, 55, 4637−4646

Scheme 1. Fabrication of Step-Growth Poly(carbonate-urea)s with Back-Biting Ring-Closing Depolymerization Ability

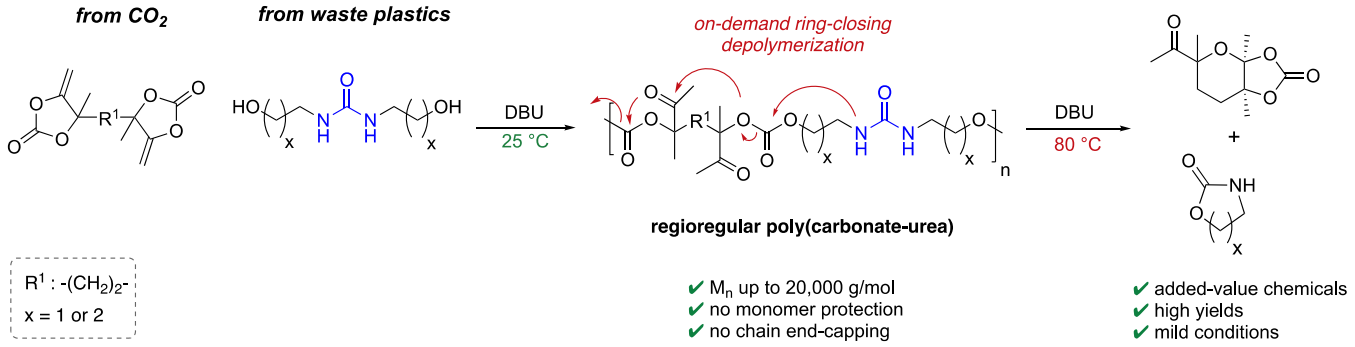

Scheme 2. Synthesis and Macromolecular Characteristics of C1P1, C1P2, and C1P3[a]

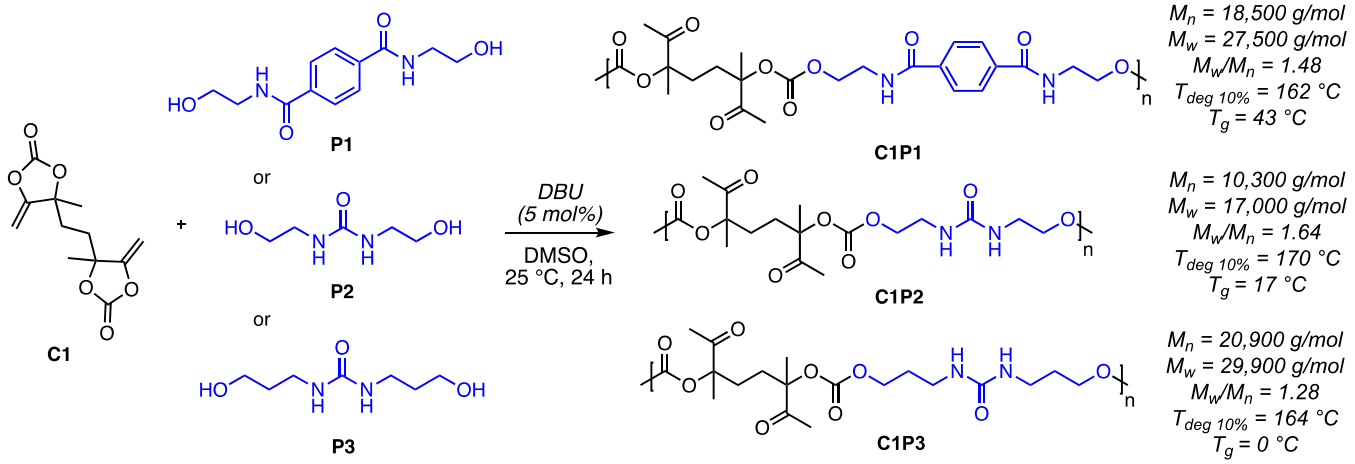

[a]Reaction conditions: [**C1**]/[**P1** or **P2** or **P3**] = 1, [C1] = 0.78 M; M_n, M_w, and M_w/M_n were determined by SEC in DMF/LiBr. Conversion >99% in all cases.

prepared by ring-opening (co)polymerization (RO(CO)-P).[9,23−30] The almost ergoneutral polymerization energetics ($\Delta G_p \approx 0$) of these RO(CO)P polymers enable chain growth below their ceiling temperature (T_c) and the (catalytic) reversion of the materials into the native three-, five-, or six-membered cyclic precursors by activated chain-end unzipping above T_c.[11,31−37] Mimicking this concept with step-growth polymers is far from trivial. Impediments to the construction of step-growth materials with ring-closing degradative ability lie in the inherent incompatibility between both chain growth and deconstruction manifolds. The inadequate microstructural polymer features also prevent the formation of well-defined cyclic molecules upon back-biting reactions in most cases. This is exemplified for polycarbonates (PCs).[38] The carbonylation of vicinal diols provides exclusively the corresponding five-membered cyclic carbonates while oligomers (minor product) coexist with six-membered trimethylene carbonates (major product) when 1,3-diols are used as templates.[28,39,40] Only 1,*x*-diols (with $x > 3$) deliver polycarbonates with decent molar masses by step-growth copolymerization, generally at high temperature to tackle the low reactivity of the comonomers and/or to eliminate the condensate (in polycondensations). However, the enlargement of the alkylene spacer between both hydroxyl units of the diols is detrimental for deconstructing the PCs via activated chain-end back-biting as the formation of seven-membered (if $x = 4$) or even larger rings is not favored. Their depolymerization into macrocyclic carbonates is now possible by transesterification (i.e., not by back-biting reaction) at elevated temperatures (235−280 °C) under vacuum distillation.[41] The chemical foundations to design PCs by step-growth polymerization with ring-closing degradative ability imposes the utilization of monomers with adequate ethylene or propylene spacers between the reactive groups but also processing conditions and adequate ceiling temperature that favor their enchainment into polymers instead of a cyclic scaffold formation. Self-immolative polymers represent an elegant solution to this issue as they can be delivered by step-growth polymerization while being prone to spontaneous disassembly via a domino fashion upon removal of a triggering moiety by an appropriate stimulus.[42−54] While interesting but rarely illustrated with polycarbonates, this class of materials suffers from (1) the utilization of protected monomers, generally not easily accessible and not sustainable, and/or (2) the stabilization of the growing chains by fast trapping of the reactive terminus to prevent a reversion, thus limiting the molar mass to short chains, which is detrimental for the thermomechanical performances of the materials.[55]

Herein, we report an original and facile methodology to fabricate polycarbonate-type polymers with cascade ring-closing depolymerization ability via an activated chain-end mechanism, delivering new cyclic scaffolds upon deconstruction. Capitalizing on our recent approach of furnishing regioregular polycarbonates by room-temperature step-growth copolymerization of exovinylene biscyclic carbonates and diols,[56−58] we envisioned that the smart skeletal editing of these PCs should solve the conflict between step-growth

https://doi.org/10.1021/acs.macromol.2c00696
Macromolecules 2022, 55, 4637−4646

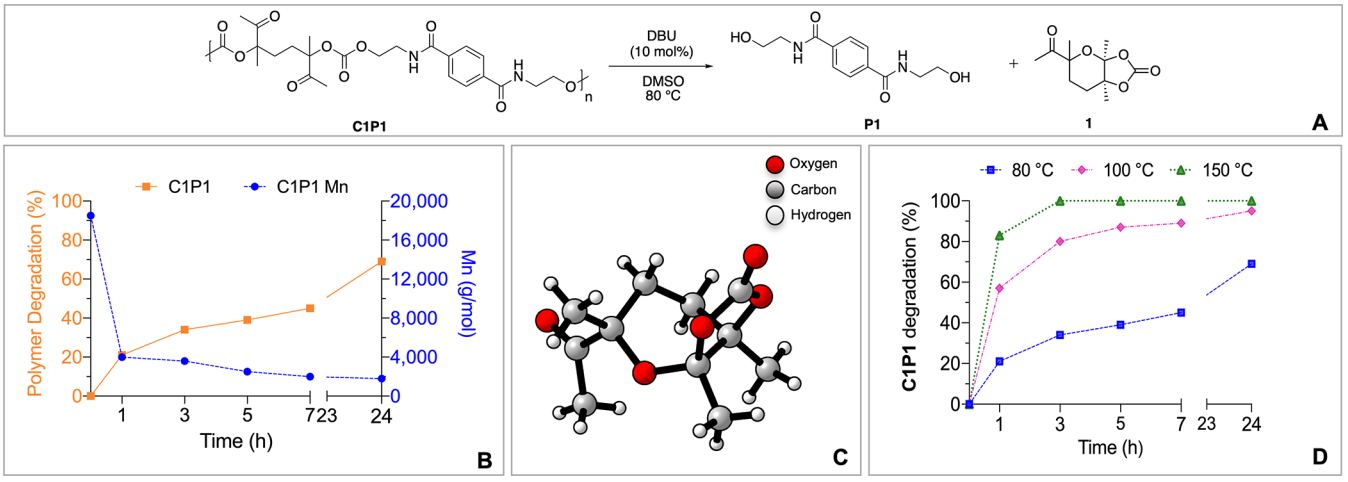

Figure 1. (A) Degradation scheme for **C1P1** and main degradation products. (B) Time evolution of the **C1P1** M_n upon deconstruction at 80 °C. (C) ORTEP representation of 5-acetyl-3a,5,7a-trimethyltetrahydro-5H-[1,3]dioxolo[4,5-*b*]pyran-2-one. (D) Time evolution of the **C1P1** degradation at 80, 100, and 150 °C. The reactions were in presence of DBU (10 mol % vs polymer repeating unit) using 1,3,5-trimethoxybenzene (TMB) as an internal standard.

copolymerization and ring-closing depolymerization. Thus, we explore the introduction of additional unprotected in-chain secondary functionalities, which are nonreactive at room temperature but activated on demand upon catalytic thermal switching (Scheme 1). The concept was validated with monomers designed from CO_2 and upcycled waste plastics, creating a sustainable and circular scenario that answers the requirements of our modern society.

RESULTS AND DISCUSSION

Design of Regioregular Poly(carbonate-amide) and Poly(carbonate-urea)s. Forging step-growth polycarbonates with ring-closing degradative ability requires engineering and unifying monomers with dual functionalities that can be activated on demand to drive selectively divergent catalytic polymerization and depolymerization pathways. To be applicable and guarantee the success of our methodology, the fine control of the polymer microstructure is capital. Errors in the enchainment of the monomers could create termination nodes stopping the depolymerization, further providing a mixture of ill-defined products. To do so, a series of polycarbonate-type polymers are synthesized by the room-temperature DBU-catalyzed step-growth copolymerization of CO_2-sourced meso-4,4′-(ethane-1,2-diyl)bis(4-methyl-5-methylene-1,3-dioxolan-2-one) (bisαCC **C1**) with waste-plastic-sourced diols containing in-chain unprotected secondary amide or urea moieties (**P1**−**3**, Scheme 2 and Figures S1−S6).[59] After 24 h, polymers **C1P1**, **C1P2**, and **C1P3** are obtained with a weight-average molar mass (M_w) of 27 500, 17 000, and 29 900 g/mol, respectively (Scheme 2, Tables S1−S3, and Figures S7−S9). The ^{1}H and ^{13}C nuclear magnetic resonance (NMR) characterizations of the three polymers (Figure S10) attest to the regioregular nature of the chains. Moreover, all resonances are in agreement with the expected copolymer microstructure with intact in-chain amide or urea linkages and pendant ketones, functionalities that are also crucial for the ring-closing deconstruction of PCs, as illustrated later, and no sign of degradation products. All polymers are isolated and display thermal stabilities with decomposition temperature at 10% weight loss ($T_{deg10\%}$) at up to 162, 170, and 164 °C for **C1P1**, **C1P2**, and **C1P3**, respectively (Scheme 2 and Figures S11−S13). All polymers are found to be amorphous by differential scanning calorimetry (DSC) (Scheme 2 and Figures S14−S16). **C1P1** displays a glass transition temperature (T_g) of 43 °C while, the T_g value decreases to 17 °C (**C1P2**) by shifting from terephthalamide segment to less rigid urea. The low T_g value of 0 °C of **C1P3** reflects its more flexible nature compared to **C1P2** due to the extension of the ethylene (in **P2**) to a propylene spacer in the structure of **P3**.

Ring-Closing Depolymerization of Poly(carbonate-amide) and Poly(carbonate-urea). **C1P1** is then subjected to deconstruction using 10 mol % of DBU (compared to the polymer repeating unit). Unlike Hammond's postulate[60] specifying that the optimal ring-closing depolymerization catalyst has to differ from the one that serves in the chain construction, we capitalized on the "master key" nature of DBU and postulated that this organobase should be also efficient for the depolymerization of our materials upon thermal switching. This hypothesis was inspired by some DBU-promoted side reactions that were observed when polycarbonates were prepared by copolymerizing **C1** with unfunctional diols (e.g., 1,4-benzenedimethanol) at 80 °C.[56] Some unexpected cyclic carbonate linkages were formed, together with the decrease in the polymer molar mass. To verify our assumption, the depolymerization of **C1P1** (containing amide linkages in the skeletal editing) is monitored by ^{1}H NMR spectroscopy, using an internal standard, to identify and quantify the degradation products and to determine the content of decomposed polymer (Figures 1A and S17). These analyses correlate with the time evolution of the SEC of the polymer highlighting the degradation profile (Figures 1B and S18). At 80 °C, 20% of **C1P1** was degraded after 1 h, with M_n that significantly dropped from 18 500 to 4000 g/mol (Figure 1B), suggesting that chain scission events rapidly split the polymer. After 24 h, ∼70% of the polymer is disassembled with some remaining oligomers of M_n = 1800 g/mol. Then, two main products are isolated and identified as the native N1,N4-bis(2-hydroxyethyl)terephthalamide **P1** (yield of 40%) and an elusive bicyclic compound **1** (yield 40%, white solid), consisting of a tetrasubstituted five-membered ethylene carbonate fused to an acetyl-substituted tetrahydropyran

https://doi.org/10.1021/acs.macromol.2c00696
Macromolecules 2022, 55, 4637−4646

Scheme 3. Effect of the Polymer Structure for Ring-Closure Depolymerization

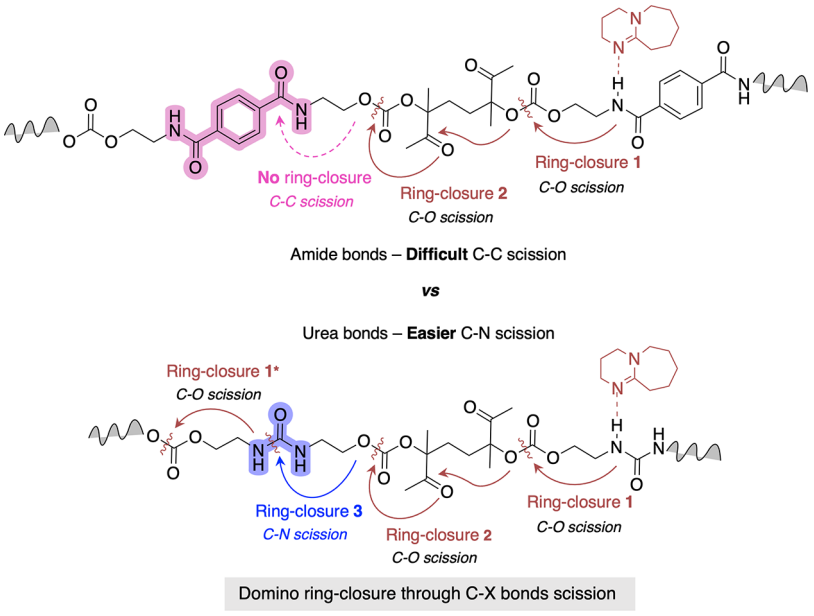

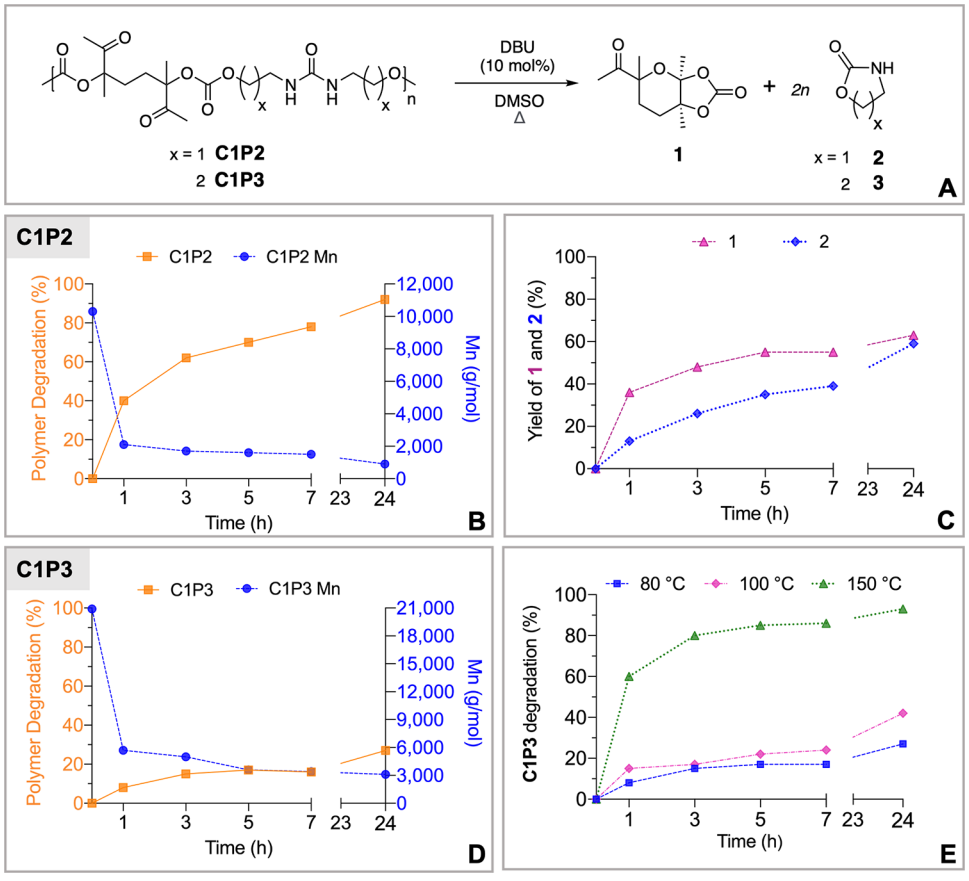

Figure 2. (A) Degradation scheme for **C1P2** and **C1P3**. (B) Evolution of polymer degradation and M_n of **C1P2** with the reaction time at 80 °C. (C) Time evolution of the **C1P2** products yields at 80 °C. (D) Time evolution of the **C1P3** M_n upon deconstruction at 80 °C. (E) Time evolution of the **C1P3** degradation at 80, 100, and 150 °C. The reactions were conducted in the presence of DBU (10 mol % vs polymer repeating unit) using 1,3,5-trimethoxybenzene (TMB) as the internal standard.

(Figures S19–S22). X-ray diffraction of the latter scaffold highlights the orientation of two methyl groups in an exclusive syn configuration, suggesting a stereoselective depolymerization process (Figures 1C and S23 and Table S4). To make the deconstruction of **C1P1** more expeditious, the depolymerization is reproduced at a higher temperature (Figures 1D, S24, and S25). At 100 °C, 95% of **C1P1** is depolymerized in 24 h and the remaining oligomers display an M_n of 1400 g/mol

https://doi.org/10.1021/acs.macromol.2c00696
Macromolecules 2022, 55, 4637–4646

Scheme 4. General Ring-Closing Depolymerization Mechanism of C1P2 Initiated by Chain Scission and Unzipping Events

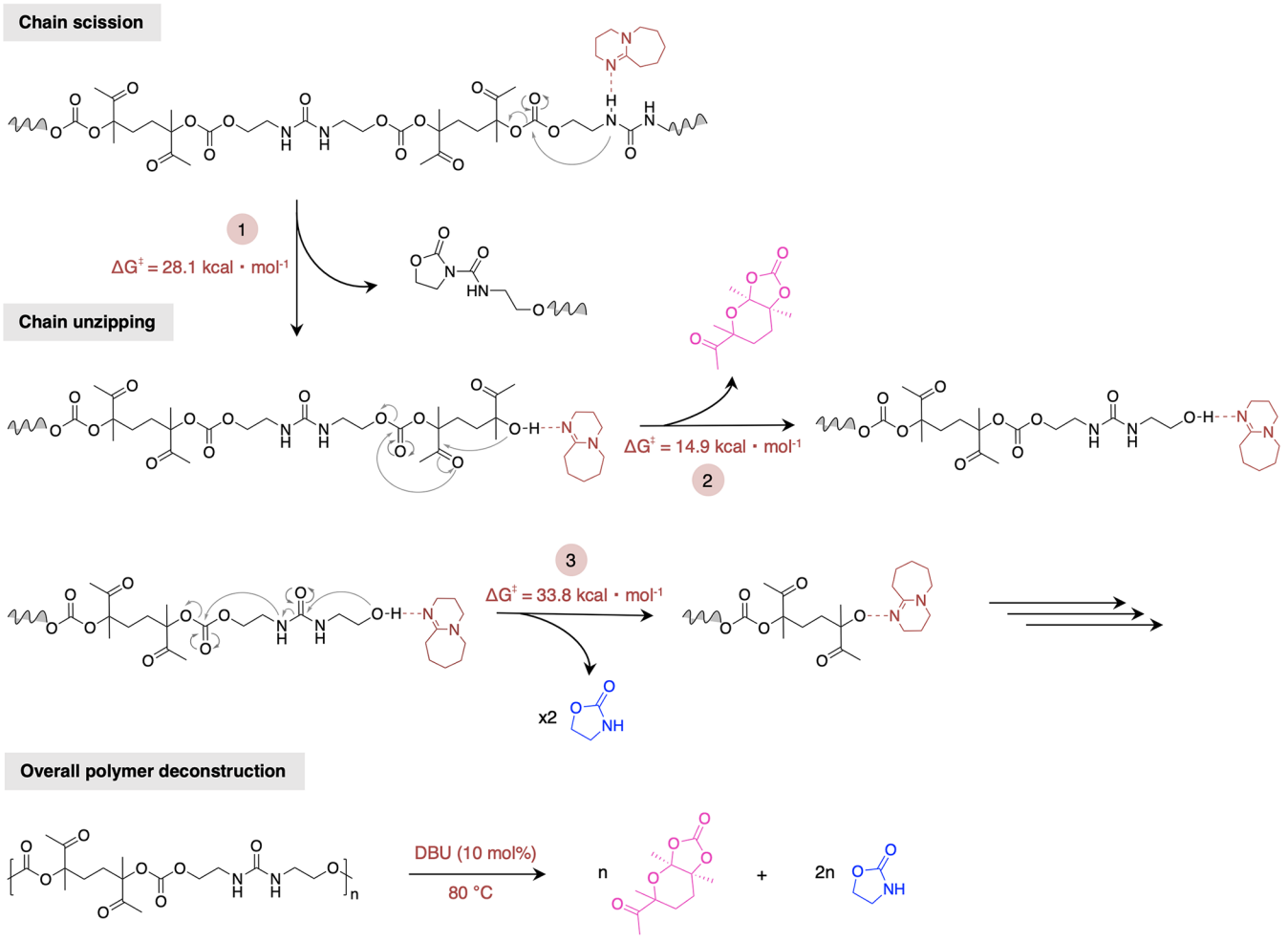

while at 150 °C, the total polymer degradation is observed within only 3 h. After 24 h, the yield of the bicyclic compound **1** significantly increases from 40% at 80 °C to 53% at 100 °C and 83% at 150 °C, confirming the beneficial effect of the temperature on the depolymerization rate. However, increasing the temperature also provides a mixture of additional cyclic co-products identified by ^{1}H NMR as N-acylated oxazolidinone and N-(2-hydroxyethyl)benzamide fragments. It suggests that besides **1** and **P1**, other products like 3,3′-terephthaloylbis-(oxazolidin-2-one) **P1a** and N-(2-hydroxyethyl)-4-(2-oxoxazolidine-3-carbonyl)benzamide **P1b** may be concomitantly formed after complete chain unzipping (Figure S24). It has to be noted that since the ^{1}H NMR signals fall in the same chemical shift, it is impossible to quantify the yield of each compound and the exact composition of the mixture (Figure S24). Every attempt to separate and isolate the various scaffolds was unsuccessful.

If the **C1P1** case validates our concept and the methodology, it furnishes a mixture of cyclic and acyclic scaffolds. This suggests that the secondary amides are not the ideal candidates to build ring-closing degradable step-growth polymers. Capitalizing on the lability of C−N linkages and the symmetry of the chemical group, we postulate that secondary ureas provide perfect substitutes to amides and totally decompose into oxazolidinones via a domino scenario (Scheme 3), pushing away the boundaries encountered with **C1P1**.

By applying analogous depolymerization protocol and characterization methodology as **C1P1**, 40% of the **C1P2** is already degraded after 1 h at 80 °C with an M_n that strongly decreases from 10 300 to 2100 g/mol and further reduces over time. After 24 h, ∼93% of the polymer is deconstructed (Figures 2A,B and S26−S28) furnishing the expected bicyclic compound **1** and the five-membered 2-oxazolidinone **2** (Figures S29 and S30) with respective yields of 63 and 59% (Figure 2C). In the absence of DBU, only 13% of the polymer is degraded at 80 °C after 24 h, with M_n that dropped from 9800 to 2900 g/mol (Figures S31 and S32). This illustrates that DBU is needed for accelerating the polymer deconstruction at this temperature.

Then, we challenged our system with **C1P3** (Figures 2A,D and S33). The presence of a propylene spacer within the polymer microstructure affects the ring-closure steps as the formation of the six-membered 1,3-oxazinan-2-one **3** is kinetically less favorable than the 5-membered one **2** from **C1P2**. As expected, during the first hours at 80 °C, the significant drop in M_n from 20 900 to 3000−5000 g/mol (Figures 2D and S34) coupled with the trace formation of the bicyclic scaffold **1** and the barely detectable **3** translates polymer fragmentation by chain scission events mainly. After 24 h, the **C1P3** degradation only reaches 27% and cyclic scaffolds **1** and **3** are produced with respective low yields of 15 and 6% (Figures S35 and S36). Increasing the degradation temperature to 100 and 150 °C is beneficial and favors the

https://doi.org/10.1021/acs.macromol.2c00696
Macromolecules 2022, 55, 4637−4646

formation of the cyclic scaffolds **1** and **3** by ring closure (Figures 2E and S37−S39). The **C1P3** degradation increases from 27% at 80 °C to 42% at 100 °C and 93% at 150 °C after 24 h of reaction (Figures 2E and S37). Concomitantly, the evolution of the SEC chromatograms toward higher elution times after 24 h (Figure S38) suggests the formation of oligomers of M_n ∼2200 g/mol at 100 °C or a "residue" with an M_n that could not be determined (out of calibration) at 150 °C as **C1P3** was almost completely deconstructed into the six-membered cyclic carbamate **3** (35% yield) and the bicyclic carbonate **1** (81% yield) (Figure S39).

We then evaluated the degradation of the most easily degradable polymer (i.e., **C1P2**) under various conditions to illustrate the robustness of the process. Dried DMSO was initially used as a solvent for our degradation studies as it is a good solvent of the polymers, and interference with water is avoided. However, in practical use, solvents always contain some water. To fit at best realistic scenarios, some water (5 wt %) is added to the reaction medium carried out at 80 °C in the presence of DBU. Similar to the reaction performed under anhydrous conditions, **C1P2** was almost fully degraded (97% vs 93%) and produced the biscyclic compound **1** in a similar yield (64% vs 63%). The oxazolidinone **2** was also obtained, however, in a lower yield (25.3% vs 59%), together with some hydrolyzed product, monomer **P2** (20.7% vs 0%) (Figure S40). **P2** is the starting monomer that may be reused in a closed-loop scenario for preparing **C1P2**. The degradation is thus operative under nonanhydrous conditions but less selective for product **2**.

If removing a high-boiling-point solvent (here, DMSO) is not straightforward and renders the practicability of the recycling process difficult, the degradation can also be carried out in low-boiling-point solvents (e.g., THF) that are easy to remove by distillation and to recycle. Although **C1P2** is insoluble in THF, 90% of the polymer is deconstructed at 80 °C after 24 h in the presence of DBU. The selectivity is however affected with a yield in **1** of 51% (vs 63% in DMSO) and 10% in **2** (vs 59% in DMSO) and more unidentified side products (Figure S41).

Lastly, we decided to evaluate the depolymerization of both **C1P1** and **C1P2** under neat (without solvent) and catalyst-free conditions. After 2 h at 150 °C, **C1P1** is fully degraded into product **1** (with a yield of 63%) and a mixture of **P1**, **P1a**, and **P1b** (Figure S42); however, the composition of this mixture is impossible to assess as previously discussed. Under these operating conditions, **C1P2** totally depolymerized as well, leading to products **1** and **2** with a yield of 76 and 67%, respectively (Figure S43). At this temperature, the depolymerizations are thus fast under attractive solvent- and catalyst-free conditions. These experiments suggest that the low degradation temperature $T_{deg10\%}$ noted for the polymers (Scheme 2) is due to their spontaneous depolymerization at this temperature. When the polymer degradation has to be realized at a rather low temperature (e.g., 80 °C), the use of the catalyst (DBU) is however absolutely needed.

Mechanistic Insights of the Poly(carbonate-urea) Formation and Depolymerization. To shed light on the depolymerization mechanism (Scheme 4) and their energetics, DFT calculations have been realized at the M062X/6-311G(d,p) level of theory and correlated with in-depth NMR characterizations and titrations. To alleviate the computational simulations and facilitate the structural elucidation of the transition states, intermediates, and final products formed during the depolymerization, all calculations have been performed on model fragments of **C1P2** mimicking the monomers, the repetitive units of the polymer, and/or the chain ends/intermediates formed upon chain scission and ring closure. A detailed discussion of the mechanisms involved for each of the DBU-catalyzed model reactions, their energy profile (in terms of Gibbs free energy), and schematic structures of the reactants, transition states, reaction intermediates, and products are given in the Supporting Information. The **C1P2** formation follows a three-step mechanism from which the tautomerization of the enol, created upon ring-opening of the exovinylidene carbonate by the alcohol moiety of **P2**, into the corresponding ketone represents the rate-determining step with an energetic penalty of 26.6 kcal·mol^{-1} (Figure S44). This value is only 1.5 kcal·mol^{-1} lower in energy than the chain scission event (Scheme 4, step 1), underlying the facile fragmentation of the polymer correlating with the rapid experimental decrease of the **C1P2** molar mass upon deconstruction. This is reflected in the barrier energy of the intramolecular nucleophilic addition of the urea NH onto the adjacent carbonate linkage (ΔG = 28.1 kcal·mol^{-1}) (Scheme 4, step 1, and Figure S45) that furnishes two polymeric fragments, one terminated by *N*-carbamoyl-oxazolidinone and the second by a hydroxyketone. Both the DFT modeling and NMR titration confirm the role of DBU in the activation of the NH groups to make them sufficiently reactive (Figures S45 and S46 and related discussion). The suggested chain termini created upon scission were further detected by ^{1}H- and ^{1}H-^{1}H-COSY NMR spectroscopy of the crude reaction mixture (Figures S47−S49) with the two correlated methylene protons at δ = 3.89 and 4.37 ppm (triplets) of the five-membered *N*-acylated moiety and the methyl signal at δ = 2.19 ppm (singlet) of the terminal hydroxyketone. This latest, whose terminal OH moiety is also activated by the organobase, initiates a double cascade cyclization furnishing the bicyclic compound **1** (Figures S50 and S51). This reaction proceeds via the creation of a 6-membered cyclic hemiacetal-type intermediate formed by the attack of the activated tertiary −OH moiety onto a neighboring ketone of the polymer skeleton that is further fused into an ethylene carbonate via a second ring-closure reaction with the adjacent carbonate linkage (Scheme 4, step 2). This double cyclization is accompanied by the concomitant release of a new polymer fragment end-capped with primary alcohol. This correlates with the presence of two NMR signals at δ = 3.05 ppm and a 3.35 ppm analogue to the signals of the 2-hydroxyethyl spacer in **P2** (Figures S47−S49). The reaction is low in energy, illustrating the ease of formation of the bicyclic structure **1**, with a rate-determining step associated with an energy barrier of only 8.6 kcal·mol^{-1} corresponding to the release of a hydroxyl-terminated PC. Finally, the polymer chain deconstruction delivers two 2-oxazolidinones **2** in a domino fashion (Figure S52). The back-biting reaction of the primary alcohol (activated by DBU) onto the carbonyl moiety of the urea linkage creates a first cyclic carbamate scaffold (Scheme 4, step 3). The vicinal off-cycle nitrogen atom is then involved in a second 2-oxazolidinone formation by a rather facile cyclization with the adjacent carbonate unit of the polymer skeleton (Scheme 4, step 3). Concomitantly, cyclization is accompanied by the release of a hydroxyketone end-capped chain that re-enters the ring-closing depolymerization loop. Due to the higher bond dissociation energy of the C−N linkages compared to the C−O ones, the oxazolidinone ring

https://doi.org/10.1021/acs.macromol.2c00696
Macromolecules 2022, 55, 4637−4646

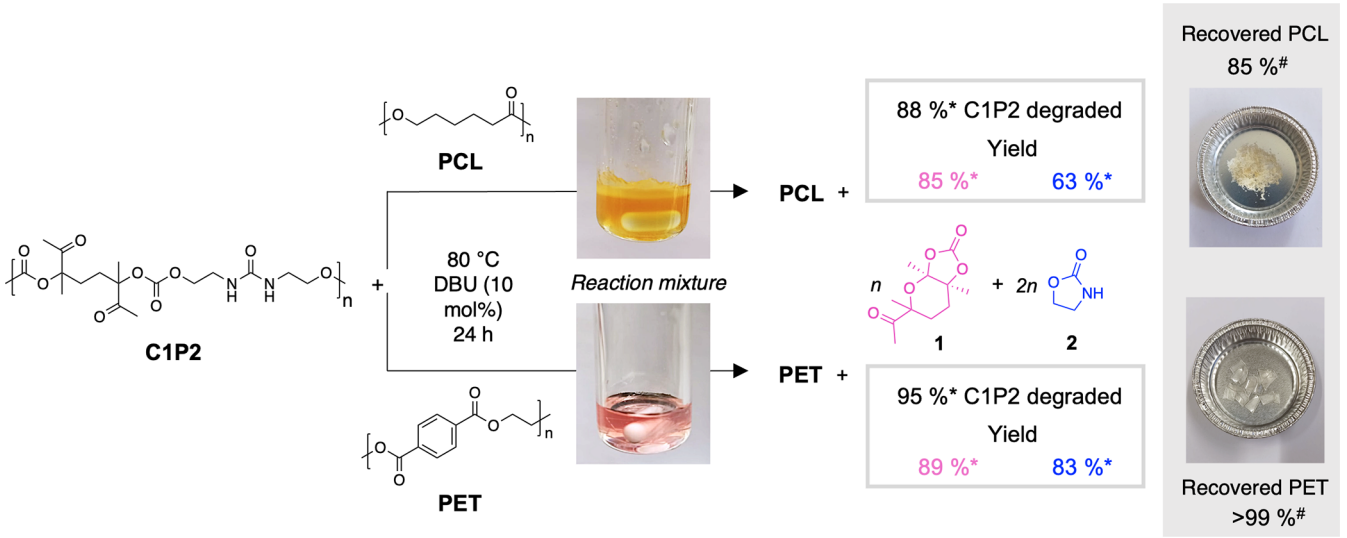

Figure 3. Selective depolymerization of **C1P2** in the presence of PCL pellets Capa 6800 or PET flakes from water bottles. *Determined by ^{1}H NMR spectroscopy on the crude product after 24 h. #Determined by weight after purification. Reactions conditions were as follows: 0.25 g of **C1P2**, 1.25 mL of DMSO, and DBU (10 mol % compared to repeating unit of polymer), and 1,3,5-trimethoxybenzene (TMB). The reactions were realized at 80 °C.

formation faces the most elevated energy barrier of 33.8 kcal·mol^{-1} and represents the rate-limiting step of the overall ring-closing depolymerization process. Such a difficulty is reflected by the experimental yields in **1** and **2** that slightly deviate from the expected theoretical value of 1/2. Ultimately, the *N*-carbamoyl-oxazolidinone chain terminus derived from the initial chain scission event is decomposed to release a last 2-oxazolidinone ring, further ensuring the total polymer deconstruction.

Selective Depolymerization of Plastic Mixtures. The (de)polymerization chemistry we have engineered offers the opportunity to program the selective degradation of mixed plastics of different nature.[16,22] To validate this rarely addressed concept, **C1P2** is mixed with two polyesters selected for their cleavable C−O bonds, i.e., either polycaprolactone (PCL), an ROP polymer prone to ring-closing depolymerization into macrocycles, solvolysis, or biodegradation in living environment, or waste polyethylene terephthalate (PET) from water bottles, a polycondensation polymer degradable by solvolysis.[11,59,61,62] Both **C1P2**/PCL and **C1P2**/PET mixed polymer formulations are then subjected to depolymerization applying the previous protocol for deconstructing pure **C1P2** (10 mol % of DBU vs polymer repeating unit, 80 °C, in DMSO) (Figure 3). With the **C1P2**/PCL mix, 88% of **C1P2** was degraded in 24 h, furnishing **1** and **2** with respective yields of 85 and 63%, while 85% of the PCL is recovered with no visible sign of degradation (Figures 3 and S53−S56). The missing 15% were lost during the purification procedure (combined dialysis and precipitation). Remarkably, PCL does not interfere in the depolymerization of **C1P2**, while the multiple intermediates with reactive −OH and −NH_2 termini created upon **C1P2** degradation do not induce trans-esterification or amidation of PCL.

Extension to the **C1P2**/PET case provides the same trend under the same conditions. Ninety-five percent of **C1P2** was deconstructed yielding **1** and **2** in 89 and 83%, respectively, without any degradation of PET that is quantitatively recovered after the separation and purification process (Figures 3 and S57).

Although unknown, building block **1** is obtained in a fully diastereoselective manner and possesses various handles for postfunctionalization. For instance, its hydroxylated tetrahydropyran core closely resembles natural products such as merulinol A.[63] Moreover, recent patents introduced the use of such type of cyclic compound with a hemiacetal cyclic carbonate template as novel electrolytes for Li-ion batteries.[64−66] Oxazolidinone **2** is of interest for drug fabrication.[67−74]

CONCLUSIONS

We have described how step-growth plastics can be edited to be easily depolymerized by cascade ring-closing approaches, offering them an attractive end-of-life scenario. Regioregular poly(carbonate-amide) and poly(carbonate-urea)s were prepared by the DBU-catalyzed step-growth copolymerization of bis-exovinylene cyclic carbonates (made from CO_2) with diols bearing unprotected secondary amide or urea linkages (made from upcycled commodity plastics) at room temperature. Upon activation by thermal switching (from 25 to 80 °C) in the presence of DBU, these groups initiated the polymer disassembly via a chain scission, followed by domino ring-closing events in DMSO. The degradation of poly(carbonate-amide) provided the native diol **P1** and a hemiacetal cyclic carbonate **1**. The depolymerization was slow at 80 °C, whereas fast and complete in a few hours at 150 °C. Substituting amide with urea was found to be beneficial, with the quasi-total depolymerization into high yields heterocycles, i.e., product **1** and oxazolidinones **2** or **3**, even at 80 °C. The process is tolerant to water and can be performed in low-boiling-point solvents that are easy to recycle (e.g., THF). Remarkably, fast and complete depolymerizations were achieved in solvent- and catalyst-free conditions at 150 °C. Lastly, poly(carbonate-urea) mixed with a common polyester (PCL or PET) was totally and selectively depolymerized, leaving intact the polyesters, further suppressing the plastics from sorting prior to recycling. Computational modeling aligns with the experimental observations and supports the fact that the polymerization occurred without competitive depolymerization and that the

https://doi.org/10.1021/acs.macromol.2c00696
Macromolecules 2022, 55, 4637−4646

polymer deconstruction proceeded by chain scission first, followed by unzipping via an activated chain-end mechanism.

As the polymers present a low degradation temperature (160−170 °C), they can be processed and used below this temperature. However, many products fulfill these requirements, e.g., coatings and foams. Our polymers might thus be utilized as polyols in polyurethane formulations to impart attractive degradation abilities to PU materials.

■ ASSOCIATED CONTENT

Supporting Information

The Supporting Information is available free of charge at https://pubs.acs.org/doi/10.1021/acs.macromol.2c00696.

Complete experimental details, additional figures, tables, and DFT protocols and calculations (PDF)

Accession Codes

CCDC 2129745 contains the supplementary crystallographic data for this paper. These data can be obtained free of charge from The Cambridge Crystallographic Data Centre via www.ccdc.cam.ac.uk/structures.

■ AUTHOR INFORMATION

Corresponding Authors

Bruno Grignard − *Center for Education and Research on Macromolecules (CERM), CESAM Research Unit, University of Liège, 4000 Liege, Belgium;* orcid.org/0000-0002-6016-3317; Email: bruno.grignard@uliege.be

Christophe Detrembleur − *Center for Education and Research on Macromolecules (CERM), CESAM Research Unit, University of Liège, 4000 Liege, Belgium;* orcid.org/0000-0001-7849-6796; Email: christophe.detrembleur@uliege.be

Authors

Fabiana Siragusa − *Center for Education and Research on Macromolecules (CERM), CESAM Research Unit, University of Liège, 4000 Liege, Belgium; Laboratoire de Chimie Organique, Service de Chimie et Physico-Chimie Organiques, Université libre de Bruxelles (ULB), 1050 Brussels, Belgium;* orcid.org/0000-0001-5744-812X

Jeremy Demarteau − *POLYMAT, University of the Basque Country UPV/EHU, 20018 Donostia-San Sebastian, Spain;* Present Address: Lawrence Berkeley National Laboratory, Berkeley, California 94720, United States

Thomas Habets − *Center for Education and Research on Macromolecules (CERM), CESAM Research Unit, University of Liège, 4000 Liege, Belgium*

Ion Olazabal − *POLYMAT, University of the Basque Country UPV/EHU, 20018 Donostia-San Sebastian, Spain*

Koen Robeyns − *Institute of Condensed Matter and Nanosciences, Université Catholique de Louvain, Louvain-La-Neuve B-1348, Belgium;* orcid.org/0000-0002-4763-4217

Gwilherm Evano − *Laboratoire de Chimie Organique, Service de Chimie et Physico-Chimie Organiques, Université libre de Bruxelles (ULB), 1050 Brussels, Belgium;* orcid.org/0000-0002-2939-4766

Raphael Mereau − *Institut des Sciences Moléculaires (ISM), UMR 5255 CNRS, Université de Bordeaux, F-33405 Talence Cedex, France;* orcid.org/0000-0002-0357-4654

Thierry Tassaing − *Institut des Sciences Moléculaires (ISM), UMR 5255 CNRS, Université de Bordeaux, F-33405 Talence Cedex, France*

Haritz Sardon − *POLYMAT, University of the Basque Country UPV/EHU, 20018 Donostia-San Sebastian, Spain;* orcid.org/0000-0002-6268-0916

Complete contact information is available at: https://pubs.acs.org/10.1021/acs.macromol.2c00696

Notes

The authors declare no competing financial interest.

■ ACKNOWLEDGMENTS

The authors from ULiege thank the "Fonds National pour la Recherche Scientifique" (F.R.S.-FNRS) and the Fonds Wetenschappelijk Onderzoek−Vlaanderen (FWO) for financial support in the frame of the EOS Project No. O019618F (ID EOS: 30902231). The authors from UPV/EHU thank the Ministry of Spain for the EUR2020-112080 financial support. FNRS is also acknowledged for financing the CO_2Switch project. This project has received funding from the European Union's Horizon 2020 research and innovation program under the Marie Skłodowska−Curie Grant Agreement No. 955700. C.D. is FNRS Research Director and thanks FNRS for financial support.

■ REFERENCES

(1) Garcia, J. M.; Robertson, M. L. The Future of Plastics Recycling. *Science* **2017**, *358*, 870−872.

(2) Zheng, J.; Suh, S. Strategies to Reduce the Global Carbon Footprint of Plastics. *Nat. Clim. Change* **2019**, *9*, 374−378.

(3) Saxon, D. J.; Gormong, E. A.; Shah, V. M.; Reineke, T. M. Rapid Synthesis of Chemically Recyclable Polycarbonates from Renewable Feedstocks. *ACS Macro Lett.* **2021**, *10*, 98−103.

(4) Fagnani, D. E.; Tami, J. L.; Copley, G.; Clemons, M. N.; Getzler, Y. D. Y. L.; McNeil, A. J. 100th Anniversary of Macromolecular Science Viewpoint: Redefining Sustainable Polymers. *ACS Macro Lett.* **2021**, *10*, 41−53.

(5) Roy, P. S.; Garnier, G.; Allais, F.; Saito, K. Strategic Approach Towards Plastic Waste Valorization: Challenges and Promising Chemical Upcycling Possibilities. *ChemSusChem* **2021**, *14*, 4007−4027.

(6) Zhao, X.; Boruah, B.; Chin, K. F.; Đokić, M.; Modak, J. M.; Soo, H. S. Upcycling to Sustainably Reuse Plastics. *Adv. Mater.* **2021**, No. 2100843.

(7) Hou, Q.; Zhen, M.; Qian, H.; Nie, Y.; Bai, X.; Xia, T.; Laiq Ur Rehman, M.; Li, Q.; Ju, M. Upcycling and Catalytic Degradation of Plastic Wastes. *Cell Rep. Phys. Sci.* **2021**, *2*, No. 100514.

(8) Worch, J. C.; Dove, A. P. 100th Anniversary of Macromolecular Science Viewpoint: Toward Catalytic Chemical Recycling of Waste (and Future) Plastics. *ACS Macro Lett.* **2020**, *9*, 1494−1506.

(9) Jehanno, C.; Pérez-Madrigal, M. M.; Demarteau, J.; Sardon, H.; Dove, A. P. Organocatalysis for Depolymerisation. *Polym. Chem.* **2019**, *10*, 172−186.

(10) Ellis, L. D.; Rorrer, N. A.; Sullivan, K. P.; Otto, M.; McGeehan, J. E.; Román-Leshkov, Y.; Wierckx, N.; Beckham, G. T. Chemical and Biological Catalysis for Plastics Recycling and Upcycling. *Nat. Catal.* **2021**, *4*, 539−556.

(11) Coates, G. W.; Getzler, Y. D. Y. L. Chemical Recycling to Monomer for an Ideal, Circular Polymer Economy. *Nat. Rev. Mater.* **2020**, *5*, 501−516.

(12) Chen, H.; Wan, K.; Zhang, Y.; Wang, Y. Waste to Wealth: Chemical Recycling and Chemical Upcycling of Waste Plastics for a Great Future. *ChemSusChem* **2021**, *14*, 4123−4136.

(13) Shieh, P.; Zhang, W.; Husted, K. E. L.; Kristufek, S. L.; Xiong, B.; Lundberg, D. J.; Lem, J.; Veysset, D.; Sun, Y.; Nelson, K. A.; Plata,

D. L.; Johnson, J. A. Cleavable Comonomers Enable Degradable, Recyclable Thermoset Plastics. *Nature* **2020**, *583*, 542−547.
(14) Shieh, P.; Nguyen, H. V. T.; Johnson, J. A. Tailored Silyl Ether Monomers Enable Backbone-Degradable Polynorbornene-Based Linear, Bottlebrush and Star Copolymers through ROMP. *Nat. Chem.* **2019**, *11*, 1124−1132.
(15) Zhu, J. B.; Watson, E. M.; Tang, J.; Chen, E. Y. X. A Synthetic Polymer System with Repeatable Chemical Recyclability. *Science* **2018**, *360*, 398−403.
(16) Christensen, P. R.; Scheuermann, A. M.; Loeffler, K. E.; Helms, B. A. Closed-Loop Recycling of Plastics Enabled by Dynamic Covalent Diketoenamine Bonds. *Nat. Chem.* **2019**, *11*, 442−448.
(17) Vora, N.; Christensen, P. R.; Demarteau, J.; Baral, N. R.; Keasling, J. D.; Helms, B. A.; Scown, C. D. Leveling the Cost and Carbon Footprint of Circular Polymers That Are Chemically Recycled to Monomer. *Sci. Adv.* **2021**, *7*, No. eabf0187.
(18) Vollmer, I.; Jenks, M. J. F.; Roelands, M. C. P.; White, R. J.; van Harmelen, T.; de Wild, P.; van der Laan, G. P.; Meirer, F.; Keurentjes, J. T. F.; Weckhuysen, B. M. Beyond Mechanical Recycling: Giving New Life to Plastic Waste. *Angew. Chem., Int. Ed.* **2020**, *59*, 15402−15423.
(19) Rahimi, A. R.; Garciá, J. M. Chemical Recycling of Waste Plastics for New Materials Production. *Nat. Rev. Chem.* **2017**, *1*, 0046.
(20) Sardon, H.; Dove, A. P. Plastics Recycling with a Difference: A Novel Plastic with Useful Properties Can Easily Be Recycled Again and Again. *Science* **2018**, *360*, 380−381.
(21) Hong, M.; Chen, E. Y. X. Chemically Recyclable Polymers: A Circular Economy Approach to Sustainability. *Green Chem.* **2017**, *19*, 3692−3706.
(22) Jehanno, C.; Demarteau, J.; Mantione, D.; Arno, M. C.; Ruipérez, F.; Hedrick, J. L.; Dove, A. P.; Sardon, H. Selective Chemical Upcycling of Mixed Plastics Guided by a Thermally Stable Organocatalyst. *Angew. Chem., Int. Ed.* **2021**, *60*, 6710−6717.
(23) Shi, C.; Li, Z. C.; Caporaso, L.; Cavallo, L.; Falivene, L.; Chen, E. Y. X. Hybrid Monomer Design for Unifying Conflicting Polymerizability, Recyclability, and Performance Properties. *Chem* **2021**, *7*, 670−685.
(24) Xiong, W.; Chang, W.; Shi, D.; Yang, L.; Tian, Z.; Wang, H.; Zhang, Z.; Zhou, X.; Chen, E. Q.; Lu, H. Geminal Dimethyl Substitution Enables Controlled Polymerization of Penicillamine-Derived β-Thiolactones and Reversed Depolymerization. *Chem* **2020**, *6*, 1831−1843.
(25) Lu, X. B.; Liu, Y.; Zhou, H. Learning Nature: Recyclable Monomers and Polymers. *Chem. − Eur. J.* **2018**, *24*, 11255−11266.
(26) Darensbourg, D. J.; Wei, S. H.; Yeung, A. D.; Ellis, W. C. An Efficient Method of Depolymerization of Poly(Cyclopentene Carbonate) to Its Comonomers: Cyclopentene Oxide and Carbon Dioxide. *Macromolecules* **2013**, *46*, 5850−5855.
(27) Deacy, A. C.; Gregory, G. L.; Sulley, G. S.; Chen, T. T. D.; Williams, C. K. Sequence Control from Mixtures: Switchable Polymerization Catalysis and Future Materials Applications. *J. Am. Chem. Soc.* **2021**, *143*, 10021−10040.
(28) Grignard, B.; Gennen, S.; Jérôme, C.; Kleij, A. W.; Detrembleur, C. Advances in the Use of CO2 as a Renewable Feedstock for the Synthesis of Polymers. *Chem. Soc. Rev.* **2019**, *48*, 4466−4514.
(29) Yuan, J.; Xiong, W.; Zhou, X.; Zhang, Y.; Shi, D.; Li, Z.; Lu, H. 4-Hydroxyproline-Derived Sustainable Polythioesters: Controlled Ring-Opening Polymerization, Complete Recyclability, and Facile Functionalization. *J. Am. Chem. Soc.* **2019**, *141*, 4928−4935.
(30) Xu, G.; Wang, Q. Chemically Recyclable Polymer Materials: Polymerization and Depolymerization Cycles. *Green Chem.* **2022**, *24*, 2321−2346.
(31) Endo, T.; Kakimoto, K.; Ochiai, B.; Nagai, D. Synthesis and Chemical Recycling of a Polycarbonate Obtained by Anionic Ring-Opening Polymerization of a Bifunctional Cyclic Carbonate. *Macromolecules* **2005**, *38*, 8177−8182.
(32) Yu, Y.; Fang, L. M.; Liu, Y.; Lu, X. B. Chemical Synthesis of CO2-Based Polymers with Enhanced Thermal Stability and Unexpected Recyclability from Biosourced Monomers. *ACS Catal.* **2021**, *11*, 8349−8357.
(33) Carrodeguas, L. P.; Chen, T. T. D.; Gregory, G. L.; Sulley, G. S.; Williams, C. K. High Elasticity, Chemically Recyclable, Thermoplastics from Bio-Based Monomers: Carbon Dioxide, Limonene Oxide and ϵ-Decalactone. *Green Chem.* **2020**, *22*, 8298−8307.
(34) Li, C.; Sablong, R. J.; van Benthem, R. A. T. M.; Koning, C. E. Unique Base-Initiated Depolymerization of Limonene-Derived Polycarbonates. *ACS Macro Lett.* **2017**, *6*, 684−688.
(35) Fahnhorst, G. W.; Hoye, T. R. A Carbomethoxylated Polyvalerolactone from Malic Acid: Synthesis and Divergent Chemical Recycling. *ACS Macro Lett.* **2018**, *7*, 143−147.
(36) Kaitz, J. A.; Lee, O. P.; Moore, J. S. Depolymerizable Polymers: Preparation, Applications, and Future Outlook. *MRS Commun.* **2015**, *5*, 191−204.
(37) Zhang, J.; Wang, L.; Liu, S.; Li, Z. Synthesis of Diverse Polycarbonates by Organocatalytic Copolymerization of CO2 and Epoxides: From High Pressure and Temperature to Ambient Conditions. *Angew. Chem., Int. Ed.* **2022**, *61*, No. e202111197.
(38) Olsén, P.; Odelius, K.; Albertsson, A. C. Ring-Closing Depolymerization: A Powerful Tool for Synthesizing the Allyloxy-Functionalized Six-Membered Aliphatic Carbonate Monomer 2-Allyloxymethyl-2-Ethyltrimethylene Carbonate. *Macromolecules* **2014**, *47*, 6189−6195.
(39) Honda, M.; Tamura, M.; Nakao, K.; Suzuki, K.; Nakagawa, Y.; Tomishige, K. Direct Cyclic Carbonate Synthesis from CO2 and Diol over Carboxylation/Hydration Cascade Catalyst of CeO2 with 2-Cyanopyridine. *ACS Catal.* **2014**, *4*, 1893−1896.
(40) Kindermann, N.; Jose, T.; Kleij, A. W. Synthesis of Carbonates from Alcohols and CO2. *Top. Curr. Chem.* **2017**, *375*, 15.
(41) Huang, J.; Olsén, P.; Svensson Grape, E.; Inge, A. K.; Odelius, K. Simple Approach to Macrocyclic Carbonates with Fast Polymerization Rates and Their Polymer-to-Monomer Regeneration. *Macromolecules* **2022**, *55*, 608−614.
(42) Baker, M. S.; Kim, H.; Olah, M. G.; Lewis, G. G.; Phillips, S. T. Depolymerizable Poly(Benzyl Ether)-Based Materials for Selective Room Temperature Recycling. *Green Chem.* **2015**, *17*, 4541−4545.
(43) Mejia, J. S.; Gillies, E. R. Triggered Degradation of Poly(Ester Amide)s via Cyclization of Pendant Functional Groups of Amino Acid Monomers. *Polym. Chem.* **2013**, *4*, 1969−1982.
(44) Dahlhauser, S. D.; Escamilla, P. R.; Vandewalle, A. N.; York, J. T.; Rapagnani, R. M.; Shei, J. S.; Glass, S. A.; Coronado, J. N.; Moor, S. R.; Saunders, D. P.; Anslyn, Ev. Sequencing of Sequence-Defined Oligourethanes via Controlled Self-Immolation. *J. Am. Chem. Soc.* **2020**, *142*, 2744−2749.
(45) Yardley, R. E.; Kenaree, A. R.; Gillies, E. R. Triggering Depolymerization: Progress and Opportunities for Self-Immolative Polymers. *Macromolecules* **2019**, *52*, 6342−6360.
(46) Sagi, A.; Weinstain, R.; Karton, N.; Shabat, D. Self-Immolative Polymers. *J. Am. Chem. Soc.* **2008**, *130*, 5434−5435.
(47) Sirianni, Q. E. A.; Gillies, E. R. The Architectural Evolution of Self-Immolative Polymers. *Polymer* **2020**, *202*, No. 122638.
(48) Kim, H.; Brooks, A. D.; Dilauro, A. M.; Phillips, S. T. Poly(Carboxypyrrole)s That Depolymerize from Head to Tail in the Solid State in Response to Specific Applied Signals. *J. Am. Chem. Soc.* **2020**, *142*, 9447−9452.
(49) Peterson, G. I.; Larsen, M. B.; Boydston, A. J. Controlled Depolymerization: Stimuli-Responsive Self-Immolative Polymers. *Macromolecules* **2012**, *45*, 7317−7328.
(50) Pal, S.; Sommerfeldt, A.; Davidsen, M. B.; Hinge, M.; Pedersen, S. U.; Daasbjerg, K. Synthesis and Closed-Loop Recycling of Self-Immolative Poly(Dithiothreitol). *Macromolecules* **2020**, *53*, 4685−4691.
(51) DeWit, M. A.; Gillies, E. R. A Cascade Biodegradable Polymer Based on Alternating Cyclization and Elimination Reactions. *J. Am. Chem. Soc.* **2009**, *131*, 18327−18334.
(52) Addy, P. S.; Shivrayan, M.; Cencer, M.; Zhuang, J.; Moore, J. S.; Thayumanavan, S. Polymer with Competing Depolymerization

Pathways: Chain Unzipping versus Chain Scission. *ACS Macro Lett.* **2020**, *9*, 855−859.
(53) Dahlhauser, S. D.; Moor, S. R.; Vera, M. S.; York, J. T.; Ngo, P.; Boley, A. J.; Coronado, J. N.; Simpson, Z. B.; Anslyn, Ev. Efficient Molecular Encoding in Multifunctional Self-Immolative Urethanes. *Cell Rep. Phys. Sci.* **2021**, *4*, No. 100393.
(54) Maschmeyer, P. G.; Liang, X.; Hung, A.; Ahmadzai, O.; Kenny, A. L.; Luong, Y. C.; Forder, T. N.; Zeng, H.; Gillies, E. R.; Roberts, D. A. Post-Polymerization 'Click' End-Capping of Polyglyoxylate Self-Immolative Polymers. *Polym. Chem.* **2021**, *12*, 6824−6831.
(55) Addy, P. S.; Shivrayan, M.; Cencer, M.; Zhuang, J.; Moore, S.; Thayumanavan, S. Polymer with Competing Depolymerization Pathways: Chain Unzipping versus Chain Scission. *ACS Macro Lett.* **2020**, *9*, 855−859.
(56) Siragusa, F.; van den Broeck, E.; Ocando, C.; Müller, A. J.; de Smet, G.; Maes, B. U. W.; de Winter, J.; van Speybroeck, V.; Grignard, B.; Detrembleur, C. Access to Biorenewable and CO2-Based Polycarbonates from Exovinylene Cyclic Carbonates. *ACS Sustainable Chem. Eng.* **2021**, *9*, 1714−1728.
(57) Gennen, S.; Grignard, B.; Tassaing, T.; Jérôme, C.; Detrembleur, C. CO2 -Sourced α-Alkylidene Cyclic Carbonates: A Step Forward in the Quest for Functional Regioregular Poly(Urethane)s and Poly(Carbonate)s. *Angew. Chem., Int. Ed.* **2017**, *56*, 10394−10398.
(58) Ngassam Tounzoua, C.; Grignard, B.; Detrembleur, C. Exovinylene Cyclic Carbonates: Multifaceted CO2-Based Building Blocks for Modern Chemistry and Polymer Science. *Angew. Chem., Int. Ed.* **2022**, *61*, No. e202116066.
(59) Demarteau, J.; Olazabal, I.; Jehanno, C.; Sardon, H. Aminolytic Upcycling of Poly(Ethylene Terephthalate) Wastes Using a Thermally-Stable Organocatalyst. *Polym. Chem.* **2020**, *11*, 4875−4882.
(60) Hammond, G. S. A Correlation of Reaction Rates. *J. Am. Chem. Soc.* **1955**, *77*, 334−338.
(61) Jehanno, C.; Pérez-Madrigal, M. M.; Demarteau, J.; Sardon, H.; Dove, A. P. Organocatalysis for Depolymerisation. *Polym. Chem.* **2019**, *10*, 172−186.
(62) Tang, X.; Chen, E. Y. X. Toward Infinitely Recyclable Plastics Derived from Renewable Cyclic Esters. *Chem* **2019**, *5*, 284−312.
(63) Choodej, S.; Teerawatananond, T.; Mitsunaga, T.; Pudhom, K. Chamigrane Sesquiterpenes from a Basidiomycetous Endophytic Fungus XG8D Associated with Thai Mangrove Xylocarpus Granatum. *Mar. Drugs* **2016**, *14*, 132.
(64) Buisine, O.; Jaunzems, J.; Kim, Y.-J.; Kasubke, M. New Components for Electrolyte Compositions. WIPO Patent WO2020025502A1, 2020.
(65) Hidaka, T.; Yamazaki, S.; Tani, A.; Kuwajima, Y. Electrolyte Solution, Electrochemical Device, Lithium Ion Secondary Battery, and Module. WIPO Patent WO2021235358A1, 2020.
(66) Kuwajima, Y.; Hidaka, T.; Kinoshita, M.; Suzuki, Y.; Shimooka, T.; Nakamura, H.; Yamada, T.; Yamazaki, S.; Yamauchi, A.; Hayashi, K.; Yamamoto, Y.; Takahashi, K. Electrolyte, Electrochemical Device, Lithium-Ion Secondary Battery, and Module. WIPO Patent WO2019220764A1, 2019.
(67) Qiu, Y.-L.; Kass, J.; Suh, B.-C.; Cao, H.; Li, W.; Peng, X.; Gao, X.; Or, Y. S.; Hepatitis, B. Antiviral Agents. WIPO Patent WO2019113175A1, 2019.
(68) Flynn, D. L.; Ahn, Y. M.; Caldwell, T.; Vogeti, L. Preparation of (Phenylamino)Pyrimidine Compounds as Autophagy Inhibitors for Treating Cancers. US Patent US20200354352A1, 2020.
(69) Sherman, D.; Cardozo, T. J. Indazole Derivatives as CaMKK2 Inhibitors and Their Preparation, Pharmaceutical Compositions and Use in the Treatment of Diseases. US Patent US20200369656A1, 2020.
(70) Bennett, F.; Imbriglio, J. E.; Kerekes, A. D.; Khan, T.; Lankin, C.; Li, D.; Wu, Z.; Xiong, Y.; Youm, H.; Yu, Y.; Kurissery, A. T.; Komanduri, V.; Ye, F. Preparation of 5,6,7,8-Tetrahydroacridine-2-Carboxamide Derivatives as Natriuretic Peptide Receptor A Agonists Useful for the Treatment of Cardiometabolic Diseases, Kidney Disease, and Diabetes. WIPO Patent WO2020236690, 2020.
(71) Nieman, J.; Hena, M.; Bai, B.; Kandadai, A. S.; Belovodskiy, A. Pyridopyrazine Derivatives as Inhibitors of Human Herpesviruses and Their Preparation. WIPO Patent WO2021174355A1, 2021.
(72) Benz, J.; Grether, U.; Hornsperger, B.; Kroll, C.; Kuhn, B.; O'Hara, F.; Richter, H. Preparation of Hexahydro-1H-Pyrido[1,2-a]Pyrazin-2-Yl Methanone Derivatives as Monoacylglycerol Lipase Inhibitors. WIPO Patent WO2021001330A1, 2021.
(73) Boisnard, S.; El-Ahmad, Y.; Fett, E.; Halley, F.; Nicolai, E.; Tabart, M.; Terrier, C.; Vivet, B. Preparation of Novel Substituted 6,7-Dihydro-5H-Benzo[7]Annulene Compounds as Inhibitors and Degraders of Estrogen Receptors. WIPO Patent WO2021063967A1, 2021.
(74) Kaldor, S. W.; Kanouni, T.; Tyhonas, J.; Murphy, E. A. N-Heteroarylphenyl Heterocyclecarboxamides as Inhibitors of RAF Kinases and Their Preparation. WIPO Patent WO2021081375A1, 2021.

https://doi.org/10.1021/acs.macromol.2c00696
Macromolecules 2022, 55, 4637−4646